

## Seiche modes of Wellington Harbour, New Zealand

EDWARD R. C. ABRAHAM

New Zealand Oceanographic Institute  
National Institute of Water & Atmospheric  
Research Ltd  
P. O. Box 14–901, Kilbirnie  
Wellington, New Zealand

**Abstract** Seiche currents were observed in Wellington Harbour, New Zealand, with an Acoustic Doppler Current Profiler (ADCP). A 600 kHz Broad-Band ADCP was deployed on the sea bed in Evans Bay in an upwards looking configuration for 20 days. The measured seiche periods were 159, 26, 17.3, and 8.3 min and there was evidence for seiching at periods of 15.8 and 14.7 min. These observations are in close agreement with the previous predictions of a finite-difference numerical model. The seiching occurred during periods of wind with speeds in excess of  $10 \text{ m s}^{-1}$ . The seiches were found to be barotropic.

**Keywords** seiches; standing waves; harbours; spectral analysis; acoustic current meters; current profiles; Wellington; New Zealand

### INTRODUCTION

Resonant standing waves, known as seiches, are often formed in enclosed bodies of water. In harbours there may be amplification at the seiche frequency of long-period broad-bandwidth waves that are incident on the harbour entrance. Tsunami (e.g., Heath 1976; Van Dorn 1984; Gilmour 1990), internal waves (e.g., Giese & Hollander 1992), pressure disturbances (e.g., Gomis et al. 1993), and surface waves (e.g., Okihiro et al. 1993) have all been reported to generate seiching. Although seiching may interfere with the day-to-day

operations of some harbours, seiche amplitudes are not normally significant. It is nevertheless important to understand the seiche characteristics of harbours which are likely to be hit by large tsunami, as amplification at the resonant frequencies may cause flooding within otherwise well-sheltered harbours.

The conventional technique for observing seiching is to monitor the associated oscillations in sea-level. Seiches may, however, have a small surface expression yet still generate observable currents. In this paper we report on the observation of seiche currents with an Acoustic Doppler Current Profiler (ADCP). This instrument provides a profile of the currents throughout the water column. Since the seiche currents are barotropic, the ADCP is well suited to distinguishing them from other baroclinic processes.

### Previous descriptions of the Wellington Harbour seiche modes

Wellington Harbour (Fig. 1), with an area of  $85 \text{ km}^2$  and a maximum width of 11 km, is situated at the southern end of the North Island of New Zealand. The Wellington area is traversed by a major fault system and is prone to large earthquakes. The biggest in recent times was in 1855 and was estimated to be of Richter magnitude 8 (Ongley 1943). The commander of a naval ship anchored in the harbour at the time reported that after the earthquake "... the tide approached and receded from the shore every 20 minutes, rising from 8 to 10 feet and receding 4 feet lower than at spring tides" (Taranaki Herald, 28 February 1855). Despite the anecdotal nature of the account it seems that oscillations with an amplitude of at least 3 m from peak to trough and a period of 20 min were observed. If such an event were to occur today it would be likely to cause severe damage along the now well-populated shoreline.

Butcher & Gilmour (1987) calculated the seiche frequencies of Wellington Harbour using the finite-difference method of Loomis (1973). The seiches were modelled as the low-frequency eigenmodes of the shallow-water wave equation:

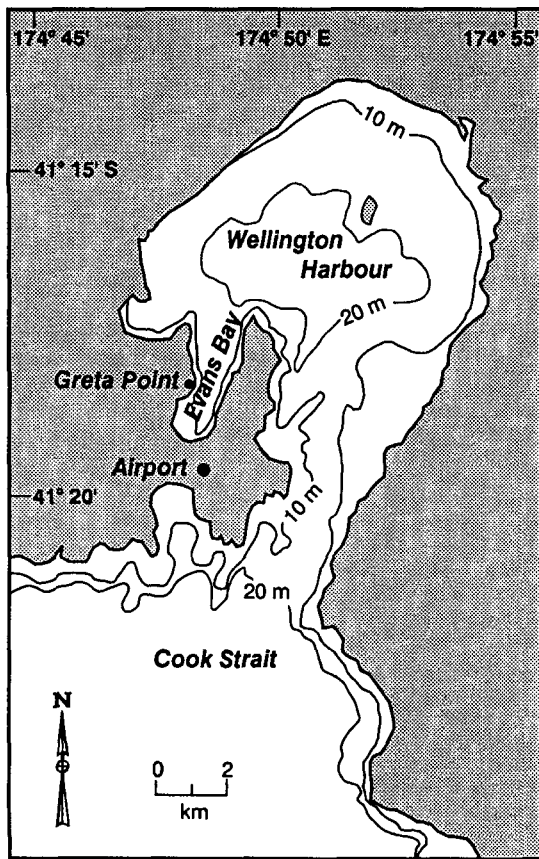


Fig. 1 Wellington Harbour, with depths shown in metres. The ADCP site was in Evans Bay, 80 m from the shore at Greta Point.

$$\nabla \cdot (h \nabla \phi) = (1/g) \partial^2 \phi / \partial t^2 \tag{1}$$

where  $h(x,y)$  is the water depth of the harbour and  $\phi(x,y,t)$  is the velocity potential. The two-dimensional current,  $v(x,y,t)$ , is given by  $v = \nabla \phi$ . Figure 2 shows the relative amplitudes of the sea-level displacements of the first six predicted resonant modes. The lowest-frequency eigenmode is a quarter-wavelength oscillation of Helmholtz type and has a period of 160 min. There is then a sequence of higher-frequency eigenmodes with wavelengths that are related to different length scales within the harbour. It is interesting to note that there are predicted modes with periods comparable to the 20-min period of the oscillations reported after the 1855 earthquake. Firmer evidence to support the existence of these simulated modes is provided by the response of the harbour to the

Pacific-wide Chilean and Alaskan tsunami of 1960 and 1964. The spectra of the tide gauge records, taken from the intervals after the tsunamis, had peaks at a period of 160 min and significant energy between periods of 25 and 31 min; there was also evidence of activity at periods around 14 min (Heath 1974, 1976; Gilmour 1990). These previous observations are in broad agreement with predictions, but the sea level measurements have to date been unable to resolve the higher-frequency seiches.

In the shallow-water approximation the two-dimensional water velocity is related to the surface displacement,  $s(x,y,t)$ , by:

$$\nabla \cdot (hv) = \frac{ds}{dt} \tag{2}$$

For a standing wave solution to Eq. 1 the velocity potential satisfies  $\phi = \phi_0 e^{i\omega t}$ , where  $\phi_0 = \phi(x,y)$  is the amplitude of the solution and  $\omega$  is its frequency. It follows, from Eq. 1 and 2, that for a seiche mode:

$$v = (-ig / \omega) \Delta s \tag{3}$$

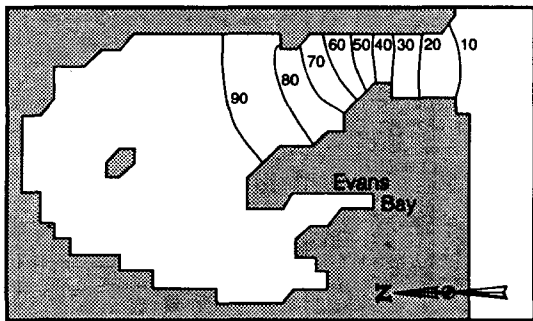
The amplitude of the seiche current is therefore proportional to the gradient of the surface displacement. Figure 2 shows that the gradient of the surface displacement of the higher-frequency modes is relatively large within Evans Bay which is thus expected to be a good site for measuring the seiche currents.

### ADCP DEPLOYMENT

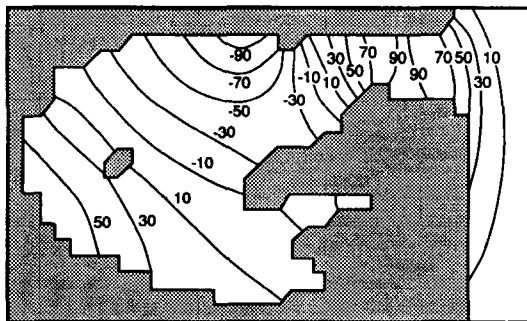
An ADCP sends acoustic pulses into the water in four beams. From the Doppler shift in the frequency of the back-scattered pulses the instrument calculates the component of the water velocity in the direction of each beam. Three components are needed to determine the water velocity; four beams enable the accuracy of the measurements to be verified. By timing the return of the pulses the instrument is able to calculate the water velocity at any distance from its transducers, within the limits of its range. A bottom-mounted ADCP, with its beams directed up into the water column, returns a vertical profile of the water currents.

The instrument used in this experiment was an RDI Broad Band ADCP with a frequency of 600 kHz. The ADCP was situated in Evans Bay, 80 m away from the Greta Point shore. The instrument was mounted in a box, which was sunk into the

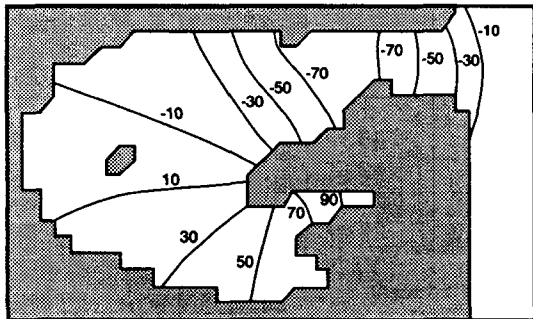
**Mode 1: 160.7 min**



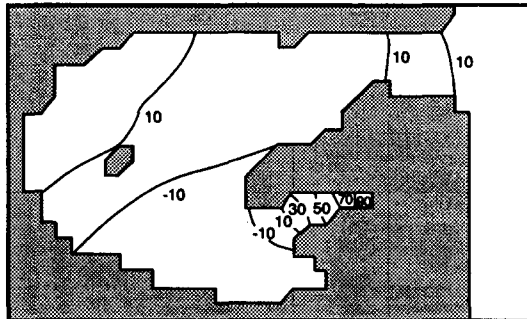
**Mode 4: 18.9 min**



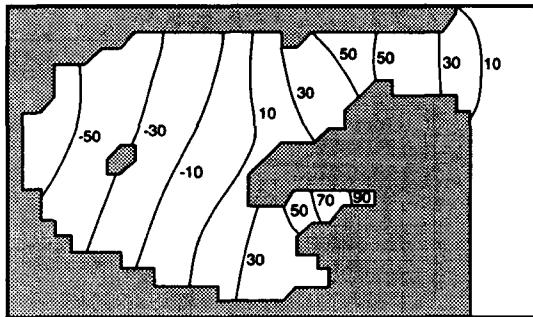
**Mode 2: 28.9 min**



**Mode 5: 17.7 min**



**Mode 3: 26.1 min**



**Mode 6: 15.7 min**

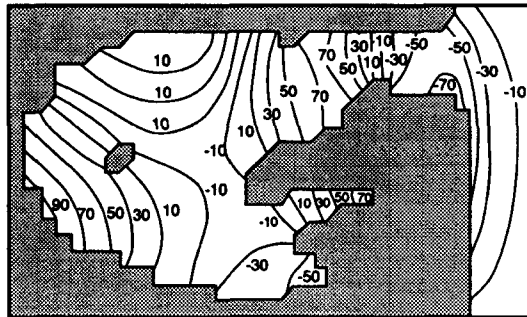


**Fig. 2** Contour charts of the relative water displacements of the six predicted resonant modes of Wellington Harbour. The displacements are expressed as a percentage of the maximum amplitude of each mode (redrawn from Butcher & Gilmour 1987).

sediment so that the transducer heads were 20 cm above the sea floor, and was connected by an underwater cable to a shore-based computer. The mean water depth at the ADCP site was 16.1 m, with a tidal range of 1.2 m. Data were received from 18 depth bins, each 75 cm high. The bottom depth bin was centred at 1.4 m above the sea bed and the upper bin at 14.2 m, 1.9 m below mean sea level. The sampling rate was set at 1.5 s with the raw data

being post-processed using RDI software to obtain 2-min averaged data. The ADCP flagged data points as bad if the velocity components from the four beams were mutually inconsistent; these bad data points were replaced by linear interpolation. The processed data are used in the subsequent analysis. The ADCP collected data continuously from 10 to 30 November 1993, apart from an 8-h gap on 19 November.

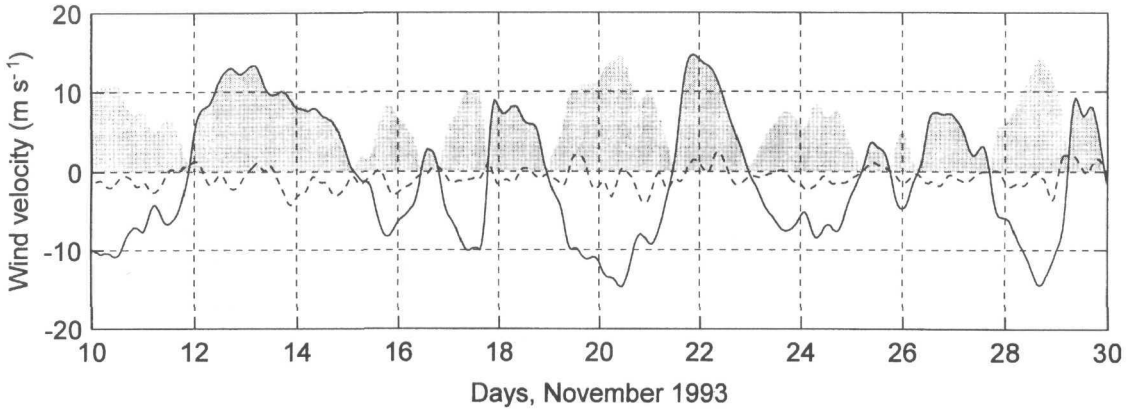


Fig. 3 Northward (solid curve) and Eastward (dashed curve) winds as measured at Wellington Airport, at the head of Evans Bay. Shading represents the corresponding wind speed.

## RESULTS AND DISCUSSION

### Observed seiche periods

The currents in Evans Bay are predominantly wind driven. During the 20-day deployment of the ADCP there were four wind events with speeds of over  $10 \text{ m s}^{-1}$  (Fig. 3). The depth-averaged currents at the ADCP site reached  $15 \text{ cm s}^{-1}$  during these events, with peak currents in excess of  $30 \text{ cm s}^{-1}$ . By comparison, the peak tidal currents, obtained by fitting the data with sinusoids of tidal frequencies, were  $< 2 \text{ cm s}^{-1}$ . Prominent seiching appears in the ADCP record as a vertically coherent, regular oscillation of the long-shore current. Figure 4 shows the long-shore current during a strong southerly on 21 November. Seiching is evident in this figure as a pronounced vertical banding. These seiche currents, with a maximum peak-to-trough magnitude of  $8 \text{ cm s}^{-1}$ , were the strongest that were observed.

To determine the seiche frequencies, spectral analyses of the long-shore and cross-shore depth-averaged currents were performed. The power spectra of both datasets were calculated and then band-averaged with a triangular window of 69 points length (0.14 cycles per h). The filter used for the band-averaging was chosen to smooth the spectra without undue smearing of the peaks. The resulting spectra are shown in Fig. 5. The confidence interval was calculated using standard techniques of spectral analysis, on the assumption that the error in the unsmoothed spectral estimate has a  $\chi^2_2$  distribution (e.g., Koopmans 1974).

In addition to measuring the currents, a bottom-mounted ADCP provides a record of the water level obtained from the travel time of the pings. Figure 6 shows the smoothed power spectrum of the depth anomaly, the tides having been previously removed.

Peaks in the long-shore current spectrum which are significant at more than the 99% confidence level are found at periods of  $26 \pm 2$ ,  $17.3 \pm 0.7$ , and  $8.3 \pm 0.2 \text{ min}$ , with the uncertainties being derived from the widths of the peaks. The two longer-period peaks are assumed to correspond to the third and fifth seiche modes, respectively. There are also two smaller peaks at  $15.8 \pm 0.6$  and  $14.7 \pm 0.5 \text{ min}$ . Although these peaks are not significant at the 99% confidence level, we shall assume that the first of these small peaks can be identified with the sixth modelled seiche mode. All of these mode identifications are based on the close agreement between the periods of the observed spectral peaks and of the modelled seiche modes (Table 1), the predicted periods of the observed modes all being within the range of the experimental uncertainty. As would be expected at a site within a narrow embayment, the seiches are not apparent in the spectrum of the cross-shore flow.

The spectrum of the depth record has a single sharp peak at a period of c. 160 min, and broader poorly defined peaks at the period of the third and fifth seiche modes (26 and 17.3 min). The other modes do not appear. From a further analysis of the spectrum, using a smoothing window only 25 points wide, the period of the sharp peak is found to be  $159 \pm 4 \text{ min}$ . This is assumed to be the

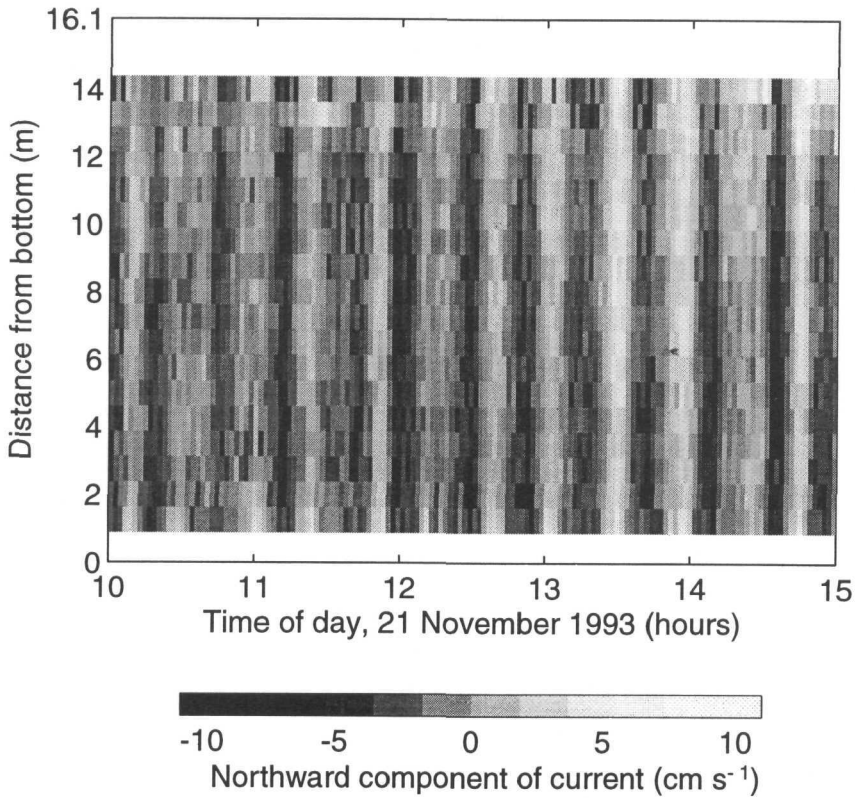


**Fig. 4** A prominent seiche event as seen by the ADCP. The figure is shaded according to the strength of the long-shore current in each depth bin, with the top of the figure being at the mean sea level. The seiching appears as a regular vertical banding.

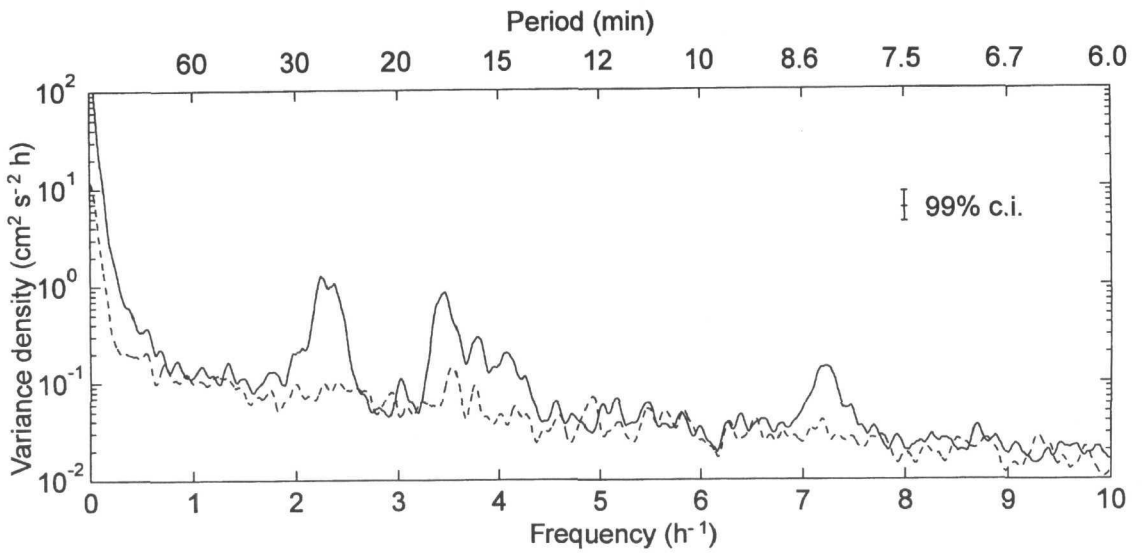


**Fig. 5** Smoothed spectra of the depth-averaged long-shore (solid) and cross-shore (dashed) currents.

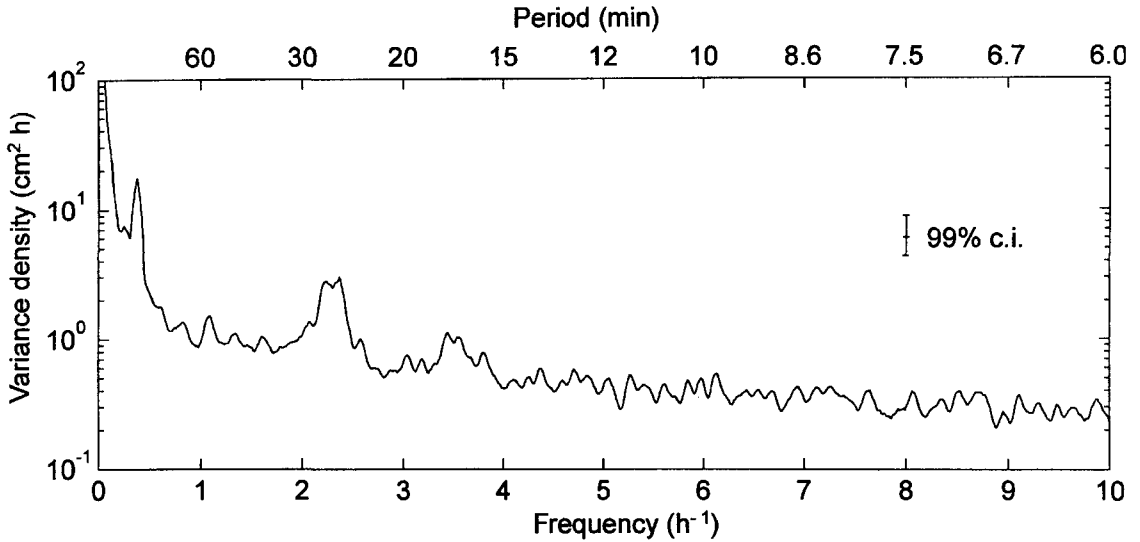


Fig. 6 Smoothed spectrum of the ADCP depth record.

frequency of the first seiche mode. It can be seen in Fig. 2 that the surface displacement associated with the first mode has a comparatively small gradient in Evan’s Bay and so it is not surprising that this mode cannot be seen in the current record.

No energy is seen at the predicted periods of the second and fourth seiche modes, in either the depth or the current record. The forcing mechanism of the seiches is not known and it is possible that these modes were not excited while the ADCP was in the water. Butcher & Gilmour (1987) did not attempt to predict the frequencies modes with periods less than 15 min, so the observation of seiching at a periods of 14.7 and 8.3 min was not anticipated.

**Vertical structure of the seiche modes**

To this point it has been tacitly assumed, through the use of the shallow-water equations and the depth-averaging of the current data, that the seiches are barotropic. The ADCP enables this assumption

to be tested. In order to study the vertical profile of the seiching, a windowed spectral analysis of the data in each depth bin is performed. Short sections of data, 128 points (4 h) long, are modulated with a raised-cosine or Von Hann window (Hamming 1977). The Fourier transform of the windowed long-shore current data is then taken, the raised-cosine window preventing undue smearing of the spectra. The complex Fourier component corresponding to periods of between 25 and 27 min is retained from the spectrum of each depth bin. Profiles are selected from times when the 26-min seiche was active (defined as when the depth-average of the chosen component has an amplitude greater than 2 cm s<sup>-1</sup>). The selected profiles of complex components are then each normalised to have zero depth-averaged phase and unit mean. The average of these normalised profiles is shown in Fig. 7, with the background shading representing their range. From Fig. 7 we see that the 26-min seiche mode is barotropic, in agreement with the previous

**Table 1** Periods of Wellington Harbour seiches.

Mode number:	1	2	3	4	5	6	7†	8†
Predicted period (min):	160.1	28.9	26.1	18.9	17.7	15.7		
Observed period (min):	159 ± 4		26 ± 2		17.3 ± 0.7	15.8 ± 0.6‡	14.7 ± 0.5‡	8.3 ± 0.2

†These mode numbers are tentative.

‡The spectral peaks at these periods were below the 99% confidence level.

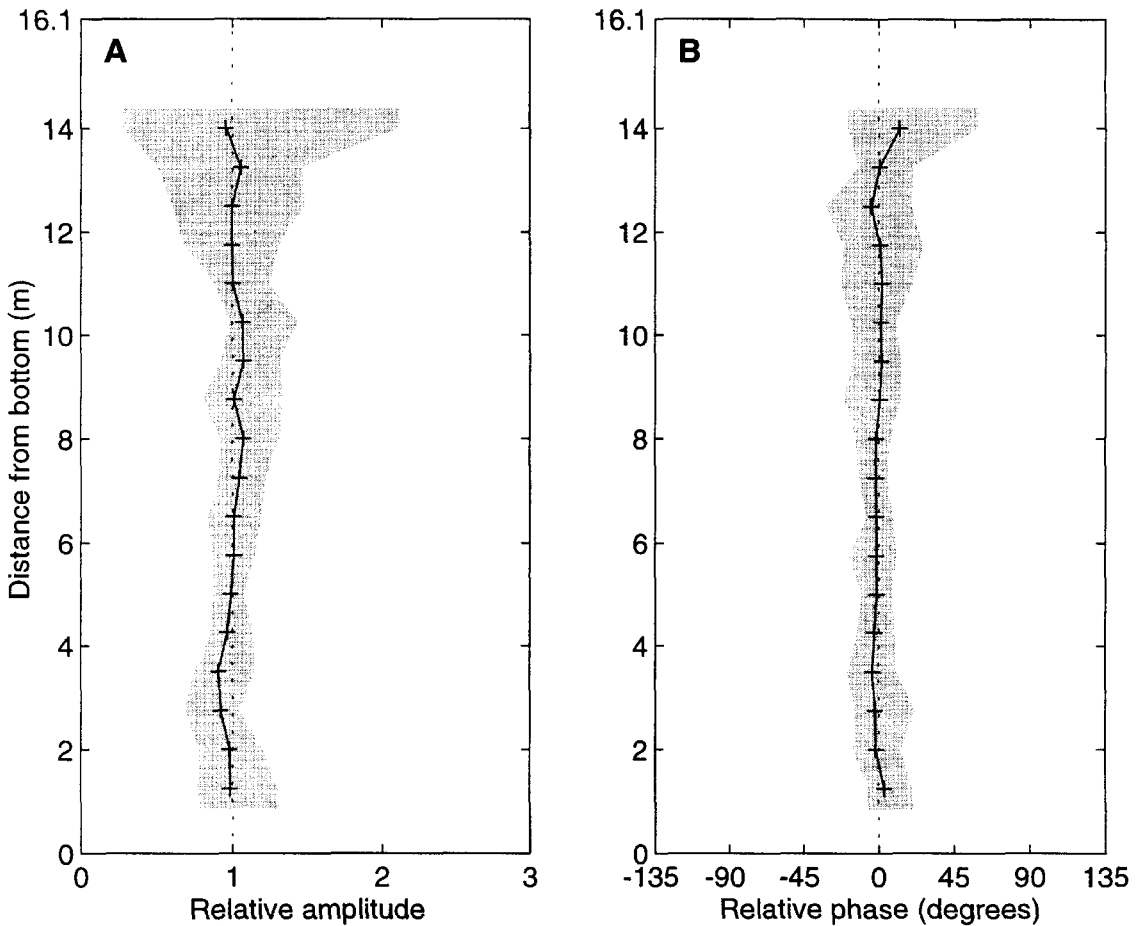


Fig. 7 Profiles of **A**, the amplitude and **B**, the phase of the average normalised 26-min seiche. Shading represents the range of the amplitude and phase of the normalised seiches. Crosses are at the centres of the depth bins.

assumption. A similar analysis at the frequencies of the 17.3 and 8.3 min modes shows that these modes are also barotropic at the site of the ADCP. This justifies the use of the depth-averaged current for the determination of the seiche frequencies.

In Evans Bay the amplitudes of the seiches are too small and their periods are too short to allow the generation of an observable bottom boundary layer. This may not be the situation throughout the harbour. The Helmholtz mode sometimes had a peak-to-trough displacement of 10 cm, one-tenth the surface displacement of the tide, and its period is approximately one-fifth of the tidal period. From a simple continuity argument it is expected that the currents associated with the Helmholtz mode may at times reach as much as half the tidal current. In Evans Bay the currents associated with this mode

are too small to be observed, however the tidal currents through the harbour entrance reach  $50 \text{ cm s}^{-1}$  (Heath 1977). A seiche with a maximum current of  $25 \text{ cm s}^{-1}$  (half the peak tidal flow) and with the 159-min period of the Helmholtz mode should allow the development of substantial vertical shear (e.g., Prandle 1982).

#### Comparison with single-bin data

Since the seiches are barotropic, the data from the ADCP may be depth-averaged without loss of information on the seiches but with a reduction in the unwanted signal from other sources. This should make the ADCP better able to resolve the seiches than a conventional current meter which only records the currents at a single depth level. The potential advantage of the ADCP over a

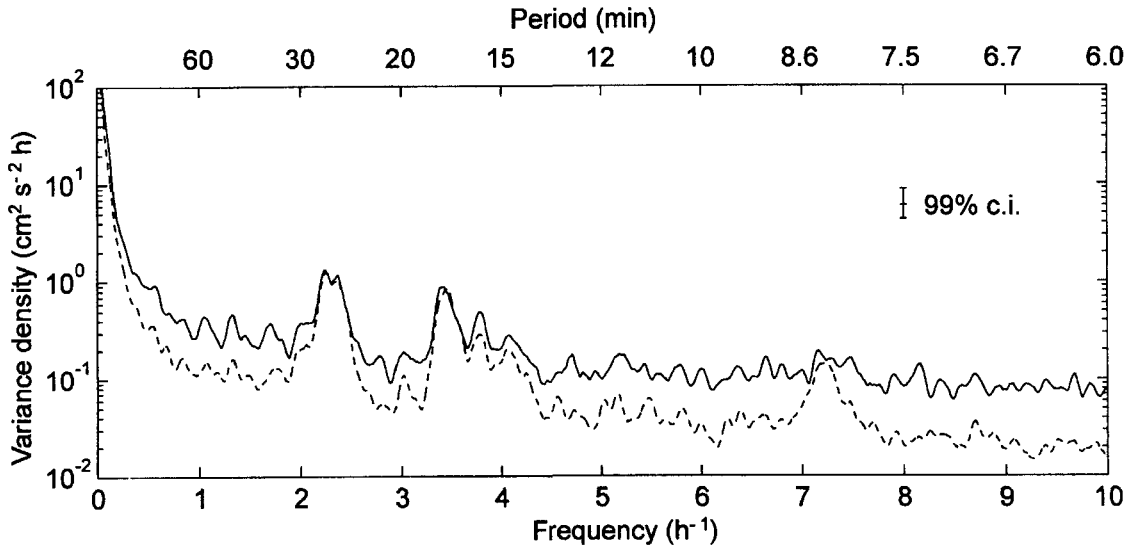


Fig. 8 Spectrum of the long-shore current data from a single depth bin (solid curve) compared with the spectrum of the depth-averaged current (dashed).

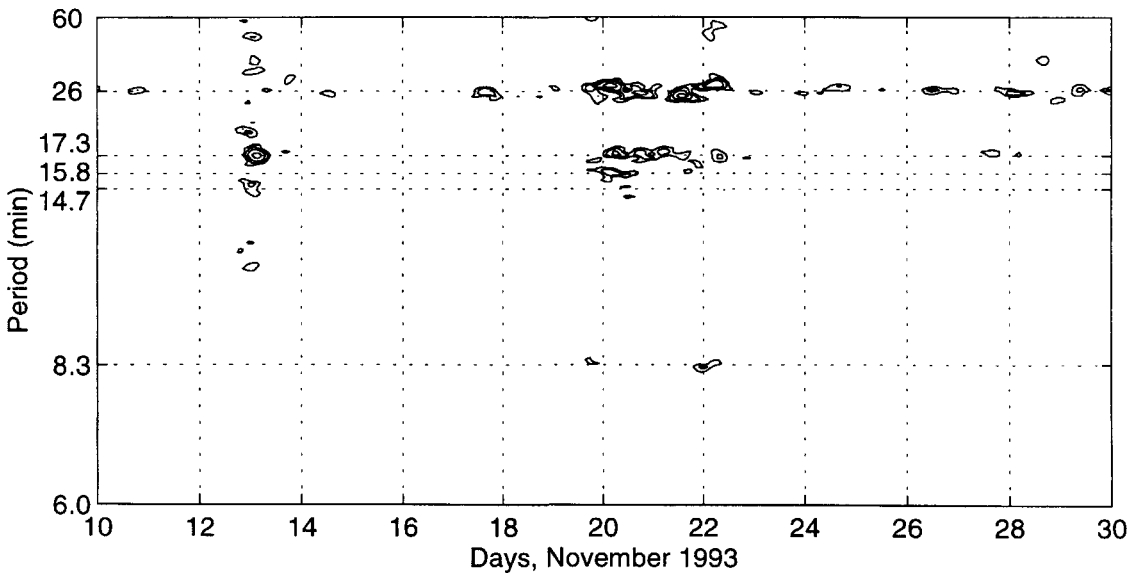
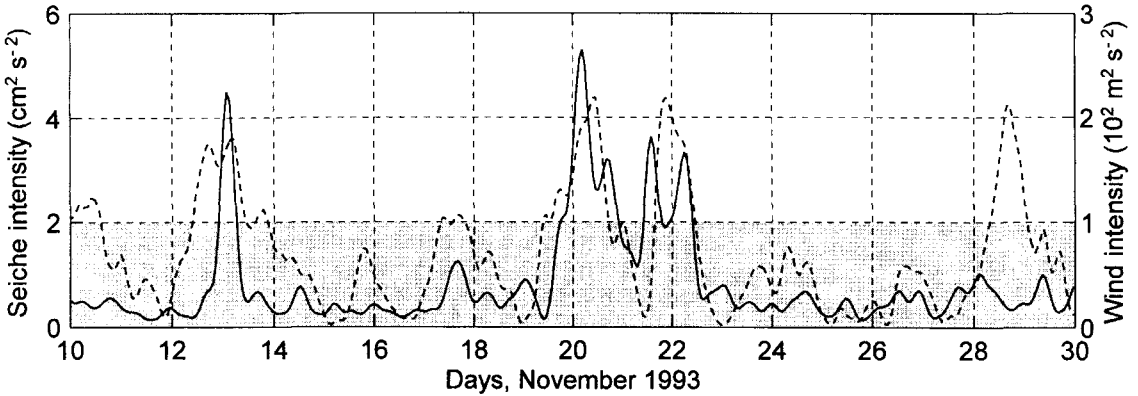


Fig. 9 Variance density of the depth-averaged long-shore current. The contours are at 2, 4, 8, and 16  $\text{cm}^2 \text{s}^{-2} \text{h}$ .

conventional current meter depends on the vertical structure of the background currents at the seiche frequencies. If the background currents in each depth bin were independent, then we would expect the background noise of the spectrum to be reduced by a factor equal to the number of depth bins. In

the worst case the background currents may themselves be barotropic: vertical averaging would not then cause any reduction of the background. Figure 8 shows the smoothed spectrum of the long-shore current from an arbitrarily chosen depth bin, centred at 9.4 m above the sea bed. The spectrum



**Fig. 10** Seiche intensity (solid curve) compared with the wind intensity (dashed) during the period of deployment of the ADCP. The shaded region represents wind speeds of less than  $10 \text{ m s}^{-1}$ .

of the depth-averaged long-shore current, from Fig. 6, is shown for comparison. The improvement in the resolution achieved by using data from throughout the water column can be seen by the reduced background of the depth-averaged spectrum. This background is a factor of 8 below the single-bin data at higher frequencies. The 8.3-min seiche could not have been resolved by a current meter which was only measuring the currents at one level in the water column.

### Time dependence of the seiches

The mechanism for the generation of the weather driven seiches is not known. Figure 9 is a contour plot showing the time dependence of the variance density of the mean long-shore current. This figure has been generated from a Von Hann windowed spectral analysis of the data, with a window length of 512 points (18 h) and with the window being shifted by 40 points (80 min) between calculations. The seiches are strongly localised in time, with no prominent seiche event lasting longer than 12 h. There are three main periods of seiche activity, centred on 13, 20, and 22 November, and these are closely associated with periods during which the wind speed was  $> 10 \text{ m s}^{-1}$  (Fig. 10). The seiche intensity has here been calculated by summing the variance density, at the seiche frequencies, of the spectra contoured in Fig. 9. The seiche modes are excited with different relative intensities under different conditions: the 17.3-min mode was strongly active on the 13th but little at other times; the 26-min mode was particularly active on the 20th

and 22nd; there was no seiching associated with the strong wind event centred on the 29th.

Attempts to correlate the seiche activity with changes in pressure measured by a meteorological station at Wellington Airport were not successful, nor did the seiching appear to be directly initiated by changes in the wind induced set-up. It may be that the seiching is being generated by long-period waves associated with the passage of the weather systems.

### ACKNOWLEDGMENTS

I am grateful to Alex Gilmour for permission to reprint Fig. 2 and I am indebted to colleagues at NIWA, particularly Jonathan Sharples and Philip Sutton, for their help with this project. The ADCP used in this experiment was obtained on loan from the Tauranga Harbour Board. The project was supported by NIWA's Non-Specific-Output-Funding programme.

### REFERENCES

- Butcher, C. N.; Gilmour, A. E. 1987: Free oscillations in Wellington and Lyttelton Harbours. *DMFS reports (NZ) 1(1)*: 1–8.
- Giese, G. S.; Hollander R. B. 1992: The relationship between coastal seiches at Palawan Island and tide-generated internal waves in the Sulu sea. *Journal of geophysical research 97(C10)*: 15573–15577.
- Gilmour, A. E. 1990: Response of Wellington Harbour to the tsunamis of 1960 and 1964. *New Zealand journal of marine and freshwater research 24*: 229–231.

- Gilmour, A. E.; Stanton, B. 1990: Tsunami Hazards in the Wellington region, *Report prepared for Wellington Regional Council by N.Z. Geological Survey*.
- Gomis, D.; Monserrat, S.; Tintoré, J. 1993: Pressure forced seiches of large amplitude in inlets of the Balearic Islands. *Journal of geophysical research* 98(C8): 14437–14445.
- Hamming, R. W. 1977: *Digital Filters*. New Jersey, Prentice-Hall, 226 p.
- Heath, R. A. 1974: Sea level oscillations in Wellington Harbour. *New Zealand journal of marine and freshwater research* 8: 403–414.
- Heath, R. A. 1976: The response of several New Zealand harbours to the 1960 Chilean Tsunami. *Tsunami Research Symposium 1974. Bulletin of the Royal Society of New Zealand* 15: 71–82.
- Heath, R. A. 1977: Circulation and hydrography of Wellington Harbour. *New Zealand Oceanographic Institute oceanographic summary* 12, 8 p.
- Koopmans, L. H. 1974: *The spectral analysis of time series*. New York, Academic, 266 p.
- Loomis, H. G. 1973: A new method for determining normal modes of irregular bodies of water with variable depth. *Hawaii Institute of Geophysics reports* HIG-73-10 (NOAA-JTRE-86).
- Okihiro, M.; Guza, R. T.; Seymour, R. J. 1993: Excitation of seiche observed in a small harbour. *Journal of geophysical research* 98(C10): 18201–18211.
- Ongley, M. 1943: Surface trace of the 1855 earthquake. *Transactions and proceedings of the Royal Society of New Zealand* 73(2): 84–89.
- Prandle, D. 1982: The vertical structure of tidal currents and other oscillatory flows. *Continental shelf research* 1(2): 191–207.
- Van Dorn, W. G. 1984: Some tsunami characteristics deducible from tide records. *Journal of physical oceanography* 14: 353–363.